

Increased Susceptibility of Thymocytes to Apoptosis in Mice Lacking AIM, a Novel Murine Macrophage-derived Soluble Factor Belonging to the Scavenger Receptor Cysteine-rich Domain Superfamily

By Toru Miyazaki,* Yumiko Hirokami,* Nobuyuki Matsuhashi,† Hisakazu Takatsuka,§ and Makoto Naito§

From the *Basel Institute for Immunology, CH-4005 Basel, Switzerland; the †Third Department of Internal Medicine, Faculty of Medicine, University of Tokyo, Bunkyo-ku, Tokyo 113-8655, Japan; and the §Second Department of Pathology, Niigata University School of Medicine, Niigata 951-8510, Japan

Summary

Apoptosis of cells must be regulated both positively and negatively in response to a variety of stimuli in the body. Various environmental stresses are known to initiate apoptosis via differential signal transduction cascades. However, induction of signals that may inhibit apoptosis is poorly understood, although a number of intracellular molecules that mediate inhibition of apoptosis have been identified. Here we present a novel murine macrophage-specific 54-kD secreted protein which inhibits apoptosis (termed AIM, for apoptosis inhibitor expressed by macrophages). AIM belongs to the macrophage scavenger receptor cysteine-rich domain superfamily (SRCR-SF), members of which share a highly homologous conserved cysteine-rich domain. In AIM-deficient mice, the thymocyte numbers were diminished to half those in wild-type mice, and CD4/CD8 double-positive (DP) thymocytes were strikingly more susceptible to apoptosis induced by both dexamethasone and irradiation *in vivo*. Recombinant AIM protein significantly inhibited cell death of DP thymocytes in response to a variety of stimuli *in vitro*. These results indicate that in the thymus, AIM functions *in trans* to induce resistance to apoptosis within DP cells, and thus supports the viability of DP thymocytes before thymic selection.

Key words: apoptosis • scavenger receptor cysteine-rich • macrophage • inhibitory factor • knockout mouse

Apoptosis, also called programmed cell death (PCD), plays a key role in the development and homeostasis of the body, in a defense mechanism, and in aging (1–4). Cells die via programmed signal cascades in the developing embryo during morphogenesis and in adults during cell turnover, thymic selection of developing thymocytes, or at the end of an immune response. Thus, apoptosis is involved in diverse physiological situations, and therefore, disturbed apoptosis may contribute to various diseases, such as cancer, autoimmunity, infections, or degenerative disorders (5–9).

Accumulating evidence has revealed that many types of environmental stress initiate apoptosis via differential signal transduction cascades (10–13). However, apoptosis must be regulated both positively and negatively in the body; identification of various intracellular elements, which appear to behave as negative regulators of apoptosis, strongly indicates the presence of inhibitory mechanisms of apoptosis

that may balance its progression (14–17). Despite the presence of these intracellular elements, induction of signals that may inhibit apoptosis is poorly understood, since we have been ignorant of the extracellular ligands that mediate inhibitory signals for apoptosis.

In this report, we present a novel murine apoptosis-inhibitory factor, termed AIM,¹ which is secreted exclusively by tissue macrophages. In AIM-deficient (AIM^{-/-}) mice, the susceptibility of thymocytes to apoptosis induced

¹Abbreviations used in this paper: AIM, apoptosis inhibitor expressed by macrophages; B6, C57Bl/6; BrdU, bromodeoxyuridine; CHO, Chinese hamster ovary; DN, double negative; DP, double positive; ES, embryonic stem; GAPDH, glyceraldehyde-3-phosphate dehydrogenase; PEC, peritoneal exudate cell; RAG, recombination activating gene; SRCR, scavenger receptor cysteine-rich; SRCR-SF, scavenger receptor cysteine-rich domain superfamily; SP, single positive; TdT, terminal deoxynucleotidyl transferase; TUNEL, TdT-mediated dUTP nick end labeling.

by various stimuli was strikingly increased. In vitro, recombinant (r)AIM protein significantly inhibited apoptosis of both thymocytes and a monocyte-derived cell line that exhibits the high binding capacity of AIM.

AIM was originally isolated as a new member of the scavenger receptor cysteine-rich domain superfamily (SRCR-SF). SRCR-SF comprises diverse molecules in a broad range of species, members of which are characterized by the presence of a unique cysteine-rich domain (SRCR domain) initially described in the type I macrophage scavenger receptor (18–20). Although the SRCR domain is highly conserved among members of the superfamily, each member appears to have different functions; thus, no consensus role for the SRCR domain has been established.

The identification of AIM will provide clues for investigating the negative regulatory systems of apoptosis via soluble factors. In addition, the apoptosis-inhibitory effect of AIM may expand the functional concept of the SRCR-SF.

Materials and Methods

cDNA Library Screening. A mouse macrophage cDNA library (Clontech) was screened with a fragment of the cysteine-rich domain of the mouse scavenger receptor cDNA (positions 1055–1390, numbered according to reference 20) which was cloned by PCR. Hybridization of the phage-transferred membrane filters was performed in $5\times$ SSC, 0.5% SDS, $5\times$ Denhardt's solution at 55°C. Hybridized membrane filters were washed in $2\times$ SSC, 0.1% SDS at 50°C for 1 h. 47 positive clones were subcloned into pBluescript SK(+) (Stratagene) and sequenced. Two of them encompassed the full-length sequence of the AIM gene.

RNA Analysis. Total RNA was isolated from various tissues of C57Bl/6 (B6) mice and adherent peritoneal exudate cells (PECs) using RNazolB solution (Tel-Test Inc.). Adherent PECs were isolated by the lavage of peritoneal cavities of thioglycollate-injected (20 mg i.p.) recombination activating gene (RAG)-2^{-/-} mice (21). 10 µg of RNA was denatured, electrophoresed on a 1% agarose gel, blotted on nylon membrane, and then hybridized with a ³²P-labeled AIM cDNA fragment.

In Situ Hybridization. Mice were perfused from heart with 4% paraformaldehyde for 30 min. Tissues were removed, then refixed in the same fixative solution for 24 h. Tissues were dehydrated in ethanol, cleared in chloroform, and then embedded in low-melting-point paraffin (Tissue Prep; Fisher Scientific). Sections were cut and mounted onto slides coated with 3-aminopropyltriethoxysilane (Aldrich Chemical Co.). Paraffin sections were subjected to in situ hybridization using digoxigenin-labeled (Boehringer Mannheim) either hybridizing (antisense) or nonhybridizing (sense) RNA probes transcribed from AIM cDNA subcloned in pBluescript SK(+) plasmid by T3 or T7 RNA polymerases. Sections were then treated with antidigoxigenin-alkaline phosphatase, and developed by 4-nitroblue tetrazolium chloride (NTB). Frozen sections from tissues were stained for pan-macrophage antigen F4/80 to evaluate AIM-expressing macrophage subpopulations.

Generation of Anti-AIM Abs. Recombinant baculovirus encoding AIM protein plus 6xHistidine-Tag was obtained by homologous recombination with pBlueBac4.5 transfer vector (Invitrogen) into which AIM cDNA fragment encoding the entire open reading frame was subcloned. The recombinant baculovirus was infected into *Trichoplusia ni* egg cells (HighFive cells; Invitro-

gen), and rAIM protein was purified from the conditioned medium by using a Histidine-Tag affinity column. Rabbits were immunized four times with purified AIM protein, and IgG subclasses including anti-AIM Abs were purified using a protein G column from rabbit serum. To generate mAbs against AIM, Balb/c mice were immunized with the rAIM described above in CFA (Sigma Chemical Co.), and spleen cells were fused with P3-X63-Ag8-U1 mouse myeloma cells by polyethylene glycol. Supernatants of hybridomas were screened by ELISA using the rAIM protein as antigen, and three positive clones (5D8, 5H7, and 3G14) were obtained. The isotype of all Abs was IgG1.

Generation of AIM^{-/-} Mice. A mouse genomic DNA clone containing exons 2–5 of the AIM gene was isolated by screening a genomic DNA library derived from the 129/sv mouse strain (Stratagene). The targeting vector was prepared using a 7-kb SpeI-BamHI fragment containing exons 2–4 of the AIM gene, pMC1-neo-polyA (Stratagene) plasmid, and the pBluescript SK(+) plasmid vector (Stratagene). This construct was designed to insert the pMC1-neo-polyA gene into the disrupted NcoI site in exon 3, which encodes the second SRCR domain. The SpeI-linearized targeting vector was electroporated into E-14.1 embryonic stem (ES) cells as described previously (22). G418-resistant clones were isolated and screened by PCR and Southern blotting. 2 out of 126 G418-resistant clones had undergone the desired homologous recombination. Positive clones were injected into B6 blastocysts, and chimeric male offspring were mated to B6 females. Mice carrying the mutation in the heterozygous state (AIM^{+/-}) were inter-crossed to produce homozygous mutants (AIM^{-/-}). 4–7-wk-old mice were used for analysis.

Serological Reagents and Flow Cytometry. Reagents used for staining T cells and subsets thereof were as described (22). Thymus, lymph node, and spleen cells were stained with saturating levels of mAbs and analyzed using a FACSCalibur[®] cytometer (Becton Dickinson).

Bromodeoxyuridine Labeling of Thymocytes. Development of DP cells was assessed by determining bromodeoxyuridine-positive (BrdU⁺) DP cells 6 and 12 h after intraperitoneal injection of 2 mg BrdU in PBS. Numbers of BrdU⁺ DP cells were evaluated by using a FACSCalibur[®] cytometer after staining thymocytes for CD4, CD8, and BrdU as described previously (23).

TUNEL Assay. The terminal deoxynucleotidyl transferase (TdT)-mediated dUTP nick end labeling (TUNEL) method is based on the specific binding of TdT to the 3'-OH ends of DNA. In brief, the periodate-lysine-paraformaldehyde (PLP)-fixed sections were covered with 2% H₂O₂ for 5 min at room temperature to inactivate endogenous peroxidase. After this time period, sections were rinsed and immersed into TdT buffer (30 mM Tris, pH 7.2, 140 mM potassium cacodylate, 1 mM calcium chloride) containing biotinylated dUTP (Bio-11-dUTP) and TdT. Sections were then nick end-labeled with biotinylated dUTP, introduced by TdT, and stained with avidin-conjugated peroxidase. Negative controls were stained by omitting TdT from the TdT buffer to ensure that endogenous peroxidase had been adequately inactivated.

AIM Transfectants and rAIM. AIM cDNA was subcloned into an expression vector, CAGGS, which contains CMV enhancer, chicken β-actin promoter, and rabbit β-globin exons and intron (24). The resulting construct (pAc-AIM) was cotransfected with pMC1-neo-polyA (Stratagene) into Chinese hamster ovary (CHO) cells by electroporation. Cells were selected by G418, and 50 resistant clones were obtained. Culture supernatant of each clone was tested for AIM protein by Western blot analysis using an anti-AIM Ab. Three clones (#12, 20, and 31) which

produced high amounts of AIM protein were used as AIM transfectants. Condition medium from these transfectants, as well as from nontransfected CHO cells as a control, was used for in vitro functional analysis of AIM. Approximate concentration of rAIM in the conditioned medium from transfectants was evaluated by Western blotting using titrated purified rAIM generated by *T. ni* egg cells as controls.

In Vitro Thymocyte Apoptosis Induction. Freshly isolated thymocytes (10^6 /well) were incubated in duplicate with various concentrations of dexamethasone in the presence of various amounts of AIM transfectant-conditioned medium. In other experiments, thymocytes were irradiated (^{137}Cs) and then incubated in the presence of various amounts of AIM transfectant-conditioned medium. To normalize any nonspecific effect potentially caused by conditioned medium, the amount of conditioned medium was equalized by adding conditioned medium from nontransfected CHO cells into wells that contained low or no amounts of conditioned medium from AIM transfectants. 20 h later, numbers of surviving DP cells were calculated by trypan blue exclusion and CD4/CD8 staining.

Binding Study. rAIM protein and a control protein (a transcription factor localized in the nucleus) were generated by recombinant baculovirus-infected *T. ni* egg cells as described above. These proteins were biotinylated using the Immunoprobe Biotinylation kit (Sigma Chemical Co.) and resuspended in PBS at 1 mg/ml. 5×10^5 J774A.1 cells were incubated with biotinylated rAIM or biotinylated control protein at 10 $\mu\text{g}/\text{ml}$ in PBS containing 5% FCS for 1 h on ice. Cells were washed twice and then incubated with streptavidin-FITC (PharMingen) for 20 min on ice. After two washes, cells were analyzed using a FACScan[®] cytometer (Becton Dickinson).

CD95/Fas-mediated Apoptosis. To induce apoptosis in J774A.1 cells, cells (10^4 /well) were incubated with 0.1 $\mu\text{g}/\text{ml}$ of cycloheximide (provided by Dr. P. Vito, Basel Institute) and various concentrations of hamster anti-mouse CD95/Fas mAb (clone Jo2; PharMingen [25]) plus rabbit mAbs cocktail anti-hamster IgG (clones G70-204 and G94-56; PharMingen), in the presence or absence of rAIM at ~ 1 ng/ml (final) for 20 h. Cell viability was measured by [^3H]thymidine incorporation in the last 4 h as described (25).

Results

Identification of a Novel Murine SRCR-SF Member Molecule, AIM. During a search for new SRCR-SF members by low-stringent screening of various cDNA libraries using the cysteine-rich domain sequence of the mouse scavenger receptor as a probe, we have isolated the cDNA for a novel murine SRCR-SF molecule, termed AIM, from a mouse macrophage cDNA library (Fig. 1 a). AIM has features of a secreted protein characterized by a potential signal-peptide sequence, and no transmembrane-like hydrophobic region (Fig. 1 a). AIM contains three SRCR domains, each of which is well conserved in other SRCR-SF members (Fig. 1 a).

Native AIM protein was immunoprecipitated from macrophage cell lysates, using anti-AIM polyclonal Abs which were generated by immunizing animals with an rAIM protein (Fig. 1 b). After SDS-PAGE, a protein of ~ 54 kD was apparent, consistent with the predicted size including N-linked glycans.

Expression Distribution of AIM Gene. The tissue distri-

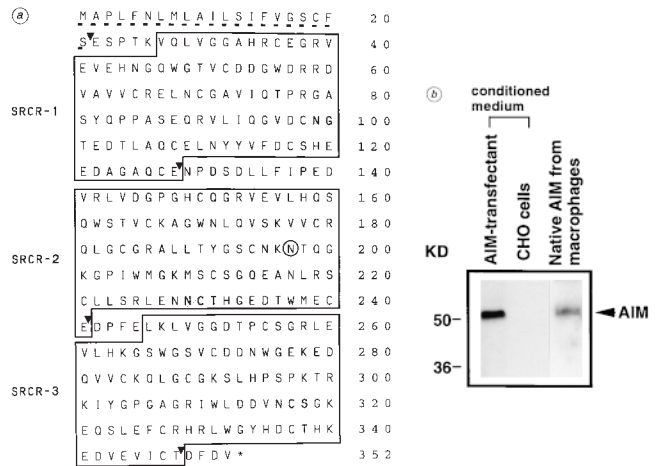


Figure 1. (a) Amino acid sequence of mouse (Balb/c strain) AIM. Dash-underlined sequence corresponds to the potential leader sequence. N-glycosylation sites (three sites) are shaded. Three SRCR domains are indicated by boxes and denoted by SRCR-1, -2, and -3. \blacktriangledown , exon-intron junctions. The aspartic acid at position 197 (circled) is serine in the 129/sv strain, based on the nucleotide substitution of adenine in the Balb/c strain to guanine in the 129/sv mouse strain. The cDNA sequence of AIM is available from EMBL/GenBank/DBJ under accession no. AF011428. (b) Peritoneal macrophages were lysed in 0.5% Triton-X buffer, and AIM protein was immunoprecipitated. Immunoprecipitating Ab was anti-AIM polyclonal rabbit Ab, which was generated by immunizing rAIM into the animal. Precipitated protein (right) as well as conditioned medium (5 μl) from either AIM-transfected CHO cells (left) or nontransfected CHO cells (middle) were size-fractionated on 10% SDS-PAGE, blotted on a membrane, and stained by anti-AIM mAb (clone 3G14). Signals were developed by the ECL system (Amersham Pharmacia Biotech).

bution of AIM gene expression was determined by Northern blot analysis. As shown in Fig. 2 a, a unique AIM mRNA of ~ 1.9 kb was expressed strongly in adherent PECs, which are mostly macrophages, and weakly in spleen and liver. The lack of a longer form suggests that no transmembrane form exists. AIM gene expression was also detected in the thymus by reverse transcription PCR (data not shown). To further characterize its expression distribution in tissues, in situ mRNA hybridization was performed on thymus, spleen, and liver tissues as well as bacillus Calmette Guérin (BCG)-induced granulomas in the liver, which harbor large numbers of infiltrating macrophages (26, 27). Interestingly, as shown in Fig. 2, b and c, macrophages at the peripheral area of granulomas, which are susceptible to environmental inflammatory stresses, express AIM. In contrast, macrophages at the central area of granulomas showed almost no AIM expression. A subpopulation of thymic macrophages in the cortex expressed AIM mRNA (Fig. 2, d and e). However, AIM expression was not detected in medullary macrophages after evaluation of numerous sections. In the spleen, AIM mRNA was expressed predominantly by macrophages in the marginal zone at the interface of the white and red pulps (Fig. 2, f and g). In the liver, strong signals were observed in a subset of, but not all, Kupffer/macrophage cells (Fig. 2, h and i). Thus, AIM gene appears to be expressed exclusively in tissue macrophages. However, in each tissue only a subpopu-

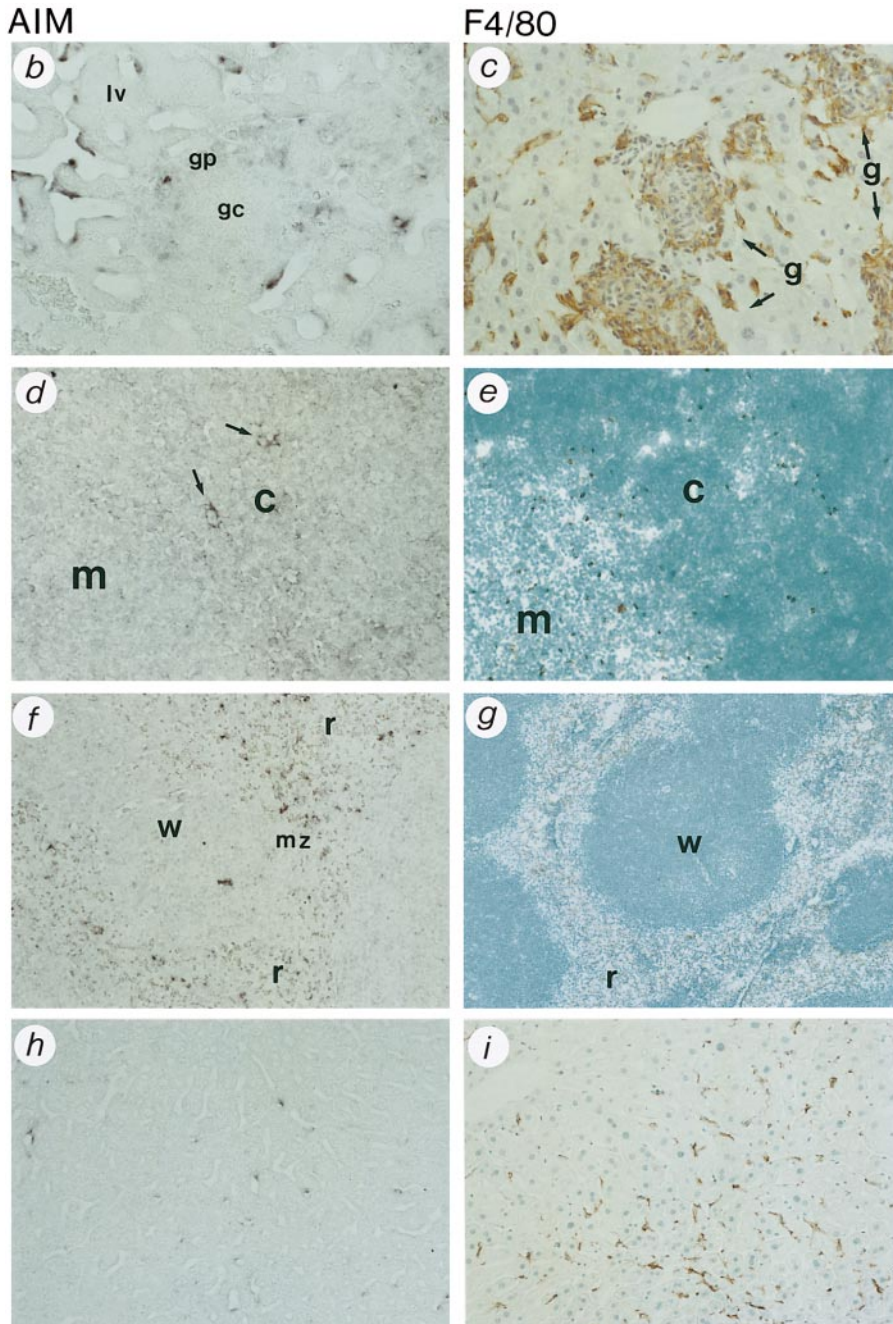
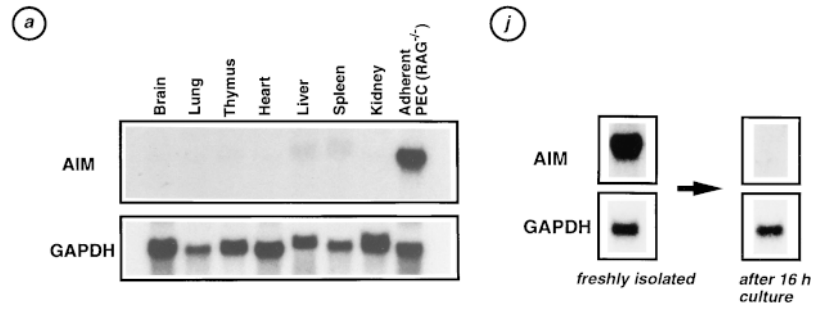


Figure 2. (a) Tissue distribution of AIM gene expression. 10 μ g of total RNA from various mouse (B6) tissues and from adherent PECs induced by thioglycollate from RAG-2^{-/-} mouse was hybridized with either AIM cDNA or glyceraldehyde-3-phosphate dehydrogenase (GAPDH) cDNA fragment. Weak background signals derived from 18S rRNA, which is slightly shorter than AIM rRNA, can be detected in every tissue. In this experiment, adherent PECs were prepared from RAG-2^{-/-} mice to avoid any contamination of T and B (B-1 and B-2) cells. However, almost comparable expression was detected in the adherent PECs from wild-type B6 mice (data not shown). (b–i) In situ hybridization analysis of AIM expression (violet/dark blue signals in b, d, f, and h) and its comparison with immunolocalization of pan-macrophage antigen, F4/80 (dark brown signals in c, e, g, and i), in mouse granulomas in the liver (b and c), thymus (d and e), spleen (f and g), and liver (h and i). (b and c) AIM is expressed in a subset of macrophages in the peripheral areas of granulomas (gp) but not in the central areas (gc). g, granulomas; lv, liver tissue. (d and e) AIM is expressed by a subpopulation of cortical macrophages as indicated by arrows (d), although macrophages exist in both cortex and medulla (e). c, cortex; m, medulla. (f and g) AIM is expressed predominantly by a subset of macrophages in the marginal zones. r, red pulp; w, white pulp; mz, marginal zone. (h and i) AIM is expressed by a subpopulation of Kupffer/macrophage cells. Original magnifications: b, $\times 400$; c, e, g, h, and i, $\times 100$; d and f, $\times 200$. (j) No AIM expression was detected in cultured macrophages. Adherent PECs were prepared from intraperitoneal thioglycollate-injected RAG-2^{-/-} mice. A portion of the cells were cultured on plastic dishes for 16 h in complete DMEM containing 10% FCS. Total RNA was prepared from freshly isolated and cultured macrophages, and hybridized with either AIM or GAPDH cDNA fragment.

lation of macrophages express AIM. This observation may reflect a requirement for specific microenvironments for AIM gene expression. This is consistent with the lack of AIM mRNA in lung, which is rich in macrophages (see Fig. 2 a). According to the AIM expression pattern in granulomas (Fig. 2, b and c), inflammatory stimuli might upregulate AIM expression in macrophages. Alternatively, cell-cell interaction between macrophages and specific types of cells in tissues might be necessary for AIM gene expression. Supporting this, freshly isolated peritoneal macrophages (which were induced by thioglycollate) expressed AIM mRNA strongly, but AIM expression disappeared completely once these cells were cultured on plastic dishes for 16 h (Fig. 2 j), and could not be reinduced by PMA, LPS, or several cytokines, including IFN- γ and interleukins (data not shown).

AIM resembles a recently reported human SRCR-SF member, Sp α , the function of which is still unknown (28), raising the possibility that AIM could be the mouse homologue of Sp α . However, since tissue distribution patterns of AIM and Sp α do not appear very similar (28), relationship between AIM and Sp α remains to be established.

Reduced Numbers of CD4/CD8 DP Thymocytes in AIM^{-/-} Mice. To gain insight into the physiological function of AIM, we produced a mouse line incapable of making AIM protein by mutating the AIM gene locus. Null mutation of the AIM gene was generated by inserting a neomycin resistance gene into exon 3, which encodes the SRCR-2 domain, via homologous recombination in ES cells (Fig. 3 a). The resulting AIM-null (AIM^{-/-}) mice were born at the expected Mendelian frequency and were apparently healthy under specific pathogen-free conditions.

However, thymi from AIM^{-/-} mice harbored significantly fewer thymocytes compared with AIM^{+/+} littermate mice ($0.68 \pm 0.2 \times 10^8$ in AIM^{-/-} vs. $1.32 \pm 0.3 \times 10^8$ in AIM^{+/+} mice; $n = 14$ each). Among the subpopulations of thymocytes dissected by CD4/CD8 surface expression, the CD4/CD8 DP thymocyte numbers in AIM^{-/-} mice were diminished to less than half the number in AIM^{+/+} mice, whereas the numbers of either CD4/CD8 DN immature thymocytes or mature single-positive (SP) thymocytes were grossly comparable in mutant and wild-type animals (Table I). Related to this, in the CD3 expression histogram of total thymocytes, the relative percentage of high CD3-expressing cells, which correspond to the mature SP thymocytes, was increased by twofold in AIM^{-/-} mice compared with AIM^{+/+} mice (Fig. 3 b). Thus, there is an exclusive decrease in DP thymocyte numbers in AIM^{-/-} mice.

Normal Thymocyte Development from the DN to the DP Stage in AIM^{-/-} Mice. To assess whether the DP cell-

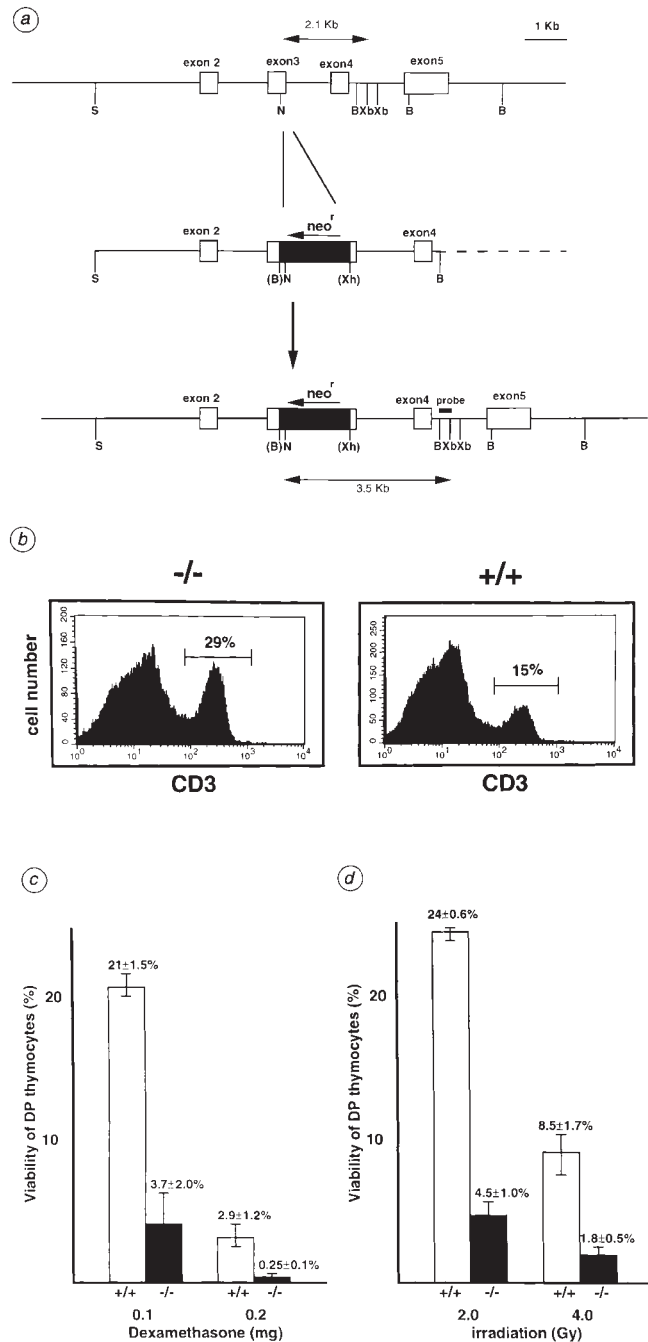


Figure 3. (a) Knockout strategy. Restriction maps are shown for the wild-type AIM gene locus (top), targeting vector (middle), and recombinant (bottom) gene locus. Exons, white boxes. neo^r, neomycin resistance gene (black box). pBluescript vector sequence, dashed line. Restriction sites: B, BamHI; N, NcoI; S, SpeI; Xb, XbaI; Xh, XhoI. Probe DNA fragment for Southern blotting is indicated, as are the 2.1- and 3.5-kb

NcoI-XbaI hybridizable fragments in wild-type and mutant DNA, respectively. (b) Thymocyte suspensions from AIM^{-/-} (-/-) and AIM^{+/+} (+/+) mice were stained for CD3 and then analyzed by flow cytometry. Histograms of CD3 expression of total thymocytes are displayed. Relative percentage of CD3^{high} population (which corresponds to mature SP thymocytes) in each type of mice is represented. (c) Apoptosis was induced in vivo in AIM^{+/+} (+/+, white boxes) and AIM^{-/-} (-/-, black boxes) mice by (c) injection of 0.1 or 0.2 mg i.p. of dexamethasone in PBS, or PBS alone, or (d) 0, 2, or 4 Gy of irradiation (¹³⁷Cs). 48 h after stimulation, mice were killed and the number of surviving DP thymocytes was determined by trypan blue exclusion and CD4/CD8 staining. Values represent the average viability of DP cells from two or three mice of each genotype and are normalized to the percentage of viable cells remaining in nonstimulated (PBS-injected, or nonirradiated) mice. Bars, SD. Three sets of experiments were performed for each stimulation, and similar results were obtained.

Table I. Absolute Numbers of Thymocyte Subpopulations

	+/+	-/-
Total	$1.32 \pm 0.3 \times 10^8$	$0.68 \pm 0.2 \times 10^8$
DP	$1.1 \pm 0.2 \times 10^8$	$0.44 \pm 0.15 \times 10^8$
CD4 ⁺ SP	$1.53 \pm 0.2 \times 10^7$	$1.32 \pm 0.2 \times 10^7$
CD8 ⁺ SP	$6.2 \pm 0.3 \times 10^6$	$6.1 \pm 0.4 \times 10^6$
DN	$4.8 \pm 0.4 \times 10^6$	$4.8 \pm 0.6 \times 10^6$

Cell numbers of each thymocyte subpopulation from AIM^{+/+} and AIM^{-/-} mice ($n = 14$ each) are presented.

specific decrease in AIM^{-/-} mice might be due to impaired kinetics of thymocyte development from the CD4/CD8 DN stage to the DP stage, we evaluated the kinetics of thymocyte maturation by biosynthetic labeling of thymocytes using BrdU in AIM^{+/+} and AIM^{-/-} mice. DN cells exhibit a high degree of cell cycling, resulting in massive proliferation of cells during development to the DP stage, whereas DP cells no longer proliferate (29). Hence, in vivo-injected BrdU is incorporated by DN cells but not by DP cells. Therefore, we evaluated BrdU⁺ subpopulations in DP cells 6 and 12 h after BrdU pulse-injection into mice to determine the generation of DP cells in these time periods. However, comparable numbers of BrdU⁺ DP cells were observed at each time point in AIM^{+/+} and AIM^{-/-} mice (4.8×10^6 in AIM^{+/+} vs. 4.5×10^6 in AIM^{-/-} after 6 h, 8.8×10^6 in AIM^{+/+} vs. 9.0×10^6 in AIM^{-/-} mice after 12 h; $n = 2$ each). This result indicates no developmental defect of thymocytes from the DN to the DP stage in AIM^{-/-} mice.

Increased Susceptibility of DP Thymocytes to Apoptosis in AIM^{-/-} Mice. An alternative explanation for the decrease of DP thymocytes is that DP cells in AIM^{-/-} mice might be more sensitive to apoptosis, resulting in increased susceptibility to death in response to environmental stimuli. In many mice with mutant apoptosis-related genes, alteration of susceptibility to apoptosis is often most apparent in the thymus (30–36), since thymocytes are highly sensitive to apoptosis (37–39). To assess the susceptibility of DP thymocytes to apoptosis in AIM^{-/-} mice, both mutant and wild-type mice were challenged in vivo with either various amounts of dexamethasone or irradiation, both of which induce massive apoptosis in thymocytes via different pathways. As shown in Fig. 3, c and d, AIM^{-/-} mice harbored far fewer numbers of surviving DP thymocytes after either stimulation than AIM^{+/+} mice, indicating a strikingly increased susceptibility of DP cells to cell death in response to both dexamethasone and irradiation in AIM^{-/-} mice. We confirmed that enhanced death of DP thymocytes in AIM^{-/-} mice after dexamethasone or irradiation treatment was due to massive apoptosis in the cortex, by the TdT-based TUNEL method (data not shown). Taken together, these results strongly indicate that AIM acts as an apoptosis-inhibitory factor in the thymus. Before positive selection,

which promotes development of DP cells to the SP cell stage, DP cells lack Bcl-2 expression (40–42) and are thus highly susceptible to apoptosis triggered by diverse environmental factors. By increasing resistance to death, AIM may augment the viability of DP cells undergoing positive selection. Perhaps related to this, the proportions of peripheral lymph node T cells expressing several TCR variable chains were different in AIM^{+/+} and AIM^{-/-} mice at statistically significant levels: $0.6 \pm 0.2\%$ in AIM^{-/-} vs. $1.8 \pm 0.4\%$ in AIM^{+/+} ($P < 0.05$) in V α 3.2⁺ CD4 cells; and $7.0 \pm 0.2\%$ in AIM^{-/-} vs. $9.2 \pm 0.4\%$ in AIM^{+/+} ($P < 0.01$) in V β 6⁺ CD4 cells ($n = 5$ each of AIM^{-/-} and AIM^{+/+} mice). In AIM^{-/-} mice, a proportion of thymocytes might fall into cell death before they are positively selected, resulting in a skew of V-chain repertoire.

Mature SP cells exhibited similar susceptibility to apoptosis induced by either dexamethasone or irradiation in AIM^{+/+} and AIM^{-/-} mice (data not shown). This is compatible with the grossly comparable numbers of SP cells in nonstimulated AIM^{+/+} and AIM^{-/-} mice (see Table I). During maturation from the DP stage to the SP stage, there is a large increase in Bcl-2 expression levels (40–42). Therefore, cell death of SP thymocytes may be predominantly inhibited by Bcl-2. When assessed by Western blotting, Bcl-2 expression levels in SP cells were similar in AIM^{+/+} and AIM^{-/-} mice (data not shown).

Thymocytes Express Normal Levels of Various Apoptosis-inhibiting and -initiating Elements in AIM^{-/-} Mice. A number of intracellular molecules have been implicated as inhibitory mediators of apoptosis. Of these, a stress-signaling kinase Sek-1 (c-Jun NH₂-terminal kinase kinase [JNKK]/mitogen-activated protein kinase kinase 4 [MKK4]) and a Bcl-2-related protein Bcl-x are expressed in DP thymocytes. Lack of either molecule in vivo caused increased susceptibility of DP cells to apoptosis in mutant mice of these genes (16, 35, 36). To assess whether the AIM-mediated inhibitory signal is related to the expression levels of these molecules, we determined protein levels of Sek-1 and Bcl-x in thymocytes from AIM^{+/+} and AIM^{-/-} mice. However, no difference was observed in mutant and wild-type mice as evaluated by Western blotting (data not shown). Since most DP thymocytes do not express Bcl-2 (40–42), possible involvement of Bcl-2 in the AIM-mediated apoptosis inhibition within DP cells can be excluded. In addition, we evaluated the expression levels of CD95/Fas (also called APO-1), TCR, and glucocorticoid receptor, all of which trigger the initiation of apoptosis in DP thymocytes. Again, no difference was observed in thymocytes from AIM^{+/+} and AIM^{-/-} mice as assessed by Western blotting and fluorocytometric analysis (data not shown).

AIM Directly Inhibits Apoptosis of DP Thymocytes. We next determined whether AIM acts directly on thymocytes as an apoptosis-inhibitory factor. We evaluated the inhibition of apoptosis of DP thymocytes by AIM in vitro by using purified thymocytes from AIM^{-/-} mice and rAIM protein generated by AIM-transfected CHO carcinoma cells. As demonstrated in Fig. 4, viability of cells after treatment

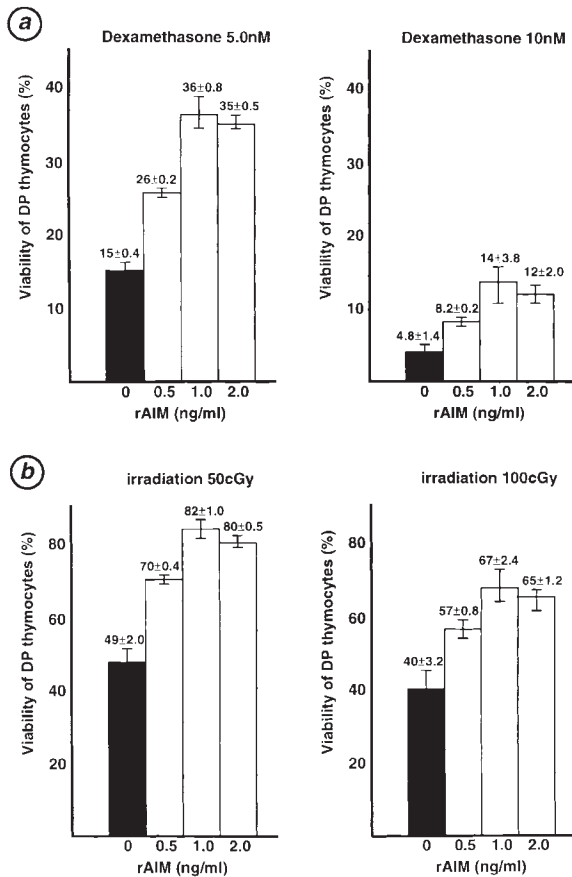


Figure 4. (a) Freshly isolated thymocytes (10^6 /well) from AIM^{-/-} mice (adherent cells, including macrophages, were depleted by cell incubation on culture plates for 30 min) were incubated with 5 or 10 nM dexamethasone in the presence of conditioned medium of AIM transfectants at indicated concentrations of rAIM (final) for 20 h. To normalize any nonspecific effect potentially caused by conditioned medium, the amount of conditioned medium was equalized by adding conditioned medium from nontransfected CHO cells into wells which contained low or no amounts of conditioned medium of AIM transfectants. (b) Thymocytes were 50 or 100 cGy irradiated and then incubated in the presence of various concentrations of rAIM as above. Surviving DP cells were calculated by trypan blue exclusion and CD4/CD8 staining. Values represent the average viability of DP cells from two independent wells and are normalized to the percentage of the DP cell numbers before culture. Bars, SD. Two sets of experiments were performed for each stimulation, and similar results were obtained.

with either dexamethasone (Fig. 4 a) or irradiation (Fig. 4 b) was improved in the presence of rAIM in a dose-dependent fashion, suggesting that the inhibition of apoptosis of DP thymocytes by AIM appears to be a direct effect. AIM did not stimulate the thymocyte proliferation that may result in a seemingly improved cell survival, as assessed by [³H]thymidine incorporation by thymocytes in the presence or absence of rAIM (data not shown).

AIM Also Inhibits CD95/Fas-mediated Apoptosis of a Monocyte-derived Cell Line. AIM appears to bind to the surface of various cell types including several cell lines, as assessed by binding studies using rAIM (Hirokami, Y., and T. Miyazaki, manuscript in preparation). Of these cells, a monocyte-derived cell line, J774A.1, showed strong bind-

ing capacity for AIM (Fig. 5 a). Therefore, by using this cell line we assessed whether the apoptosis-inhibitory effect of AIM is restricted to thymocytes or may be more general. Since J774A.1 cells express high cell surface levels of CD95/Fas antigen (Fig. 5 b), we induced apoptosis within J774A.1 cells by CD95/Fas cross-linking in combination with cycloheximide (43) in the presence or absence of rAIM in vitro, and determined their viability. As demonstrated in Fig. 5 c, the presence of rAIM again improved cell viability after treatment with different concentrations of anti-CD95/Fas Ab. This result strongly suggests that AIM may inhibit apoptosis not only of thymocytes but also

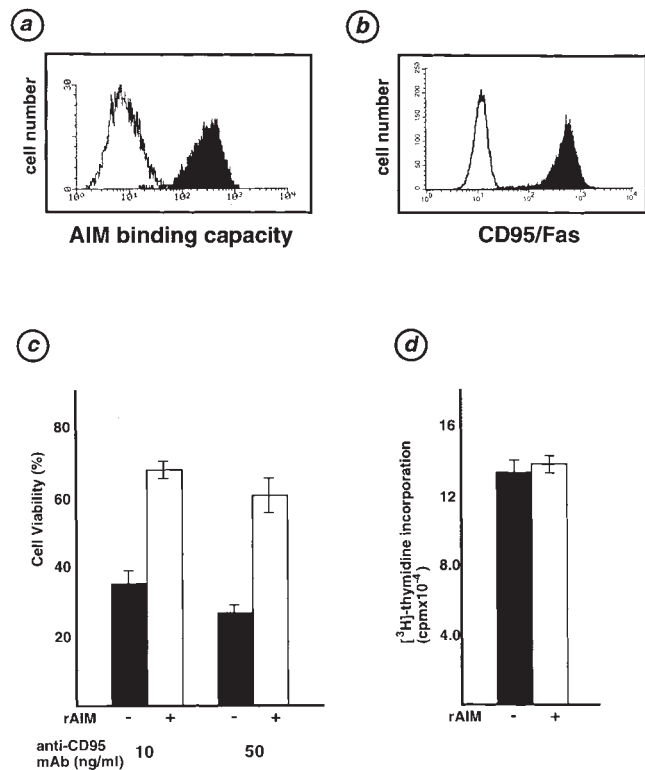


Figure 5. (a) AIM binding capacity of J774A.1 cells is presented as log fluorescence by black histograms, and the control protein bindings that are regarded as backgrounds are represented by white histograms. (b) CD95/Fas expression on the surface of J774A.1 cells. Cells were incubated with 50 μ g/ml of mouse IgG for 15 min on ice to block nonspecific binding of Abs via Fc receptors. Cells were washed once, stained with FITC-conjugated anti-CD95/Fas (clone Jo2), and then analyzed by flow cytometry. White histogram, unstained cells as a control. (c) J774A.1 cells (10^4 /well) were cultured with various concentrations of hamster anti-CD95/Fas mAb plus rabbit mAbs cocktail anti-hamster IgG and 0.1 μ g/ml of cycloheximide, in the presence (~ 1 ng/ml; white boxes, +) or absence (black boxes, -) of rAIM. After 16 h of culture, [³H]thymidine (1 μ Ci/well) was pulsed, and cells were further incubated for 4 h and then harvested. Values represent the average [³H]thymidine incorporation from three independent wells and are normalized to the percentage of the incorporation observed without Abs. Bars, SD. Three sets of experiments were performed for each stimulation, and similar results were obtained. (d) J774A.1 cells (10^4 /well) were cultured for 16 h in the presence or absence of rAIM, but without anti-CD95 mAb and cycloheximide. Cells were pulsed with [³H]thymidine (1 μ Ci/well), further incubated for 4 h, and then harvested. Values represent the average [³H]thymidine incorporation from three independent wells. Bars, SD.

of a spectrum of target cells to which AIM binds. In addition, inhibition of CD95/Fas-mediated death by AIM, together with inhibition of either dexamethasone- or irradiation-induced thymocyte apoptosis, demonstrates that AIM induces resistance to multiple initiations of apoptosis. Treatment of J774A.1 with rAIM in culture did not alter the cell surface CD95/Fas expression levels (data not shown), excluding rescue of cells by AIM from apoptosis by downregulation of CD95/Fas expression. In addition, rAIM did not modulate the proliferation of J774A.1 cells as assessed by [³H]thymidine incorporation in the absence of anti-CD95 mAb (and cycloheximide; Fig. 5 d), indicating that the improved cell viability observed in the presence of rAIM was certainly due to the inhibition of death as in the case of thymocytes.

Discussion

AIM, a Novel Apoptosis Inhibitory Factor. In this report, we described a novel murine secreted protein that inhibits apoptosis; AIM appears to increase resistance to multiple initiations of apoptosis. AIM was originally identified as a new member of the SRCR-SF. However, no other SRCR-SF member is known to be involved in the inhibition of apoptosis, reflecting the diverse functions of SRCR-SF member molecules.

The inhibition of apoptosis of purified DP thymocytes by rAIM in vitro clearly demonstrated that AIM directly functions on DP thymocytes. These in vitro experiments using purified thymocytes and rAIM exclude the possibilities that (a) AIM might be a counter-ligand for receptors that promote apoptosis, and thus might work as an antagonist of other apoptosis-regulating factors in the thymus; and (b) AIM might alter the recognition threshold at which macrophages engulf cells undergoing apoptosis and, as a consequence, AIM^{-/-} mice might have fewer surviving cells after stimuli that induce apoptosis.

However, the molecular mechanism of the inhibitory effect mediated by AIM remains to be established. According to the comparable levels of apoptosis-initiating molecules (CD95/Fas, TCR, glucocorticoid receptor) and intracellular apoptosis-inhibiting elements (Bcl-x, Bcl-2, Sek-1) in thymocytes of AIM^{-/-} and AIM^{+/+} mice, AIM appears to inhibit apoptosis of cells not simply by modulating the expression of these known apoptosis-related molecules, but by mediating an independent signaling cascade.

Two Independent Modes of Thymocyte Protection from Apoptosis. AIM-mediated inhibition of apoptosis within DP thymocytes revealed two major physiological modes for protecting thymocytes from death in the thymus. In the cortex, AIM is secreted by a subset of macrophages, and

functions in trans to decrease DP thymocyte susceptibility to apoptosis, thus protecting DP cells from death until they are positively selected. In contrast, in the medulla, Bcl-2 expression is upregulated in SP cells after positive selection, and induces strong resistance to apoptosis within SP cells themselves (40–42). This model appears to be consistent with the observations by Kyewski and colleagues demonstrating that a subset of cortical macrophages form “rosettes” with DP cells in the thymus (44, 45), and that the DP thymocytes associated with these macrophages are selectively protected from either spontaneous or experimentally induced apoptosis both in vivo and in vitro (46; and Kyewski, B.A., unpublished observations). It may be possible that in the thymus, subsets of cortical macrophages have the advantage of associating with DP thymocytes, perhaps via chemoattractants or ligation of surface molecules, and thus support the viability of associated DP cells via AIM. The skewing of several TCR V-chain repertoires in AIM^{-/-} mice might reflect unscheduled death of a proportion of thymocytes undergoing positive selection caused by the lack of AIM, which may augment their viability before selection. However, further studies are required to investigate more precisely the influence of AIM on T cell repertoire formation. Interestingly, macrophages also induce death within DP thymocytes via MHC-TCR interactions or by secreting various effectors (47). Hence, macrophages might balance the progression of apoptosis of DP thymocytes by differentially mediating either positive or negative signals depending on microenvironmental stimuli.

AIM Functions on a Variety of Cell Types. Inhibition of apoptosis of J774A.1 cells by AIM in vitro suggests that the apoptosis-inhibitory effect of AIM is more general; AIM could be involved in the negative regulation of apoptosis, not only of DP thymocytes but also of other types of cells in the body to which AIM binds, in the specific microenvironments where AIM expression is induced in macrophages. For instance, AIM might play important roles at inflammatory and infectious sites, according to the following observations by in situ analysis: (a) AIM expression appears to be increased in activated macrophages at inflammatory sites; and (b) in the spleen, AIM is predominantly expressed by macrophages in the marginal zone, which are highly susceptible to blood-borne pathogen exposure. It is established that apoptosis of both effector hematopoietic cells and target cells is involved in the progression of inflammation and infectious disease (3, 4). Therefore, AIM might balance the apoptosis of these cells by its inhibitory effect, thus regulating progression of the disease. Further characterization of AIM particularly by using AIM^{-/-} mice will clarify the in vivo roles in some pathological situations of the negative regulation of apoptosis directed by macrophages.

We are grateful to Drs. J. Pieters, J.F. McBlane, M. Colonna, P. Vito, R. Torres, and S. Gilfillan for critical reading of the manuscript and discussions; Dr. B.A. Kyewski for kind permission to cite unpublished results; U. Müller for ES cell injections; and E. Wagner, W. Metzger, and R. Zedi for help with the mice.

The Basel Institute for Immunology was founded and is supported by F. Hoffman-La Roche Ltd. (Basel, Switzerland).

Address correspondence to Toru Miyazaki, The Basel Institute for Immunology, Grenzacherstrasse 487, postfach CH-4005, Basel, Switzerland. Phone: 41-61-605-1303; Fax: 41-61-605-1364; E-mail: miyazaki@bii.ch

Received for publication 6 October 1998.

References

1. Steller, H. 1995. Mechanisms and genes of cellular suicide. *Science*. 267:1445–1449.
2. Jacobson, M.D., M. Weil, and M.C. Raff. 1997. Programmed cell death in animal development. *Cell*. 88:347–354.
3. Raff, M.C. 1992. Social controls on cell survival and cell death. *Nature*. 356:397–400.
4. Vaux, D.L., G. Haeccker, and A. Strasser. 1994. An evolutionary perspective on apoptosis. *Cell*. 76:777–779.
5. Thompson, C.B. 1995. Apoptosis in the pathogenesis and treatment of disease. *Science*. 267:1456–1462.
6. Cory, S. 1995. Regulation of lymphocyte survival by the bcl-2 gene family. *Annu. Rev. Immunol.* 13:513–543.
7. Yang, E., and S.J. Korsmeyer. 1996. Molecular thanatopsis: a discourse on the BCL2 family and cell death. *Blood*. 88:386–401.
8. Strasser, A., D.C. Huang, and D.L. Vaux. 1997. The role of the bcl-2/ced-9 gene family in cancer and general implications of defects in cell death control for tumourigenesis and resistance to chemotherapy. *Biochim. Biophys. Acta*. 1333: F151–F178.
9. Chao, D.T., and S.J. Korsmeyer. 1998. BCL-2 family: regulators of cell death. *Annu. Rev. Immunol.* 16:395–419.
10. Minden, A., A. Lin, M. McMahon, C. Lange-Carter, B. Derijard, R.J. Davis, G.L. Johnson, and M. Karin. 1994. Differential activation of ERK and JNK mitogen-activated protein kinases by Raf-1 and MEKK. *Science*. 266:1719–1723.
11. Pombo, C.M., J.V. Bonventre, J. Avruch, J.R. Woodgett, J.M. Kyriakis, and T. Force. 1994. The stress-activated protein kinases are major c-Jun amino-terminal kinases activated by ischemia and reperfusion. *J. Biol. Chem.* 269:26546–26551.
12. Westwick, J.K., A.E. Bielawska, G. Dbaibo, Y.A. Hannun, and D.A. Brenner. 1995. Ceramide activates the stress-activated protein kinases. *J. Biol. Chem.* 270:22689–22692.
13. Verheij, M., R. Bose, X.H. Lin, B. Yao, W.D. Jarvis, S. Grant, M.J. Birrer, E. Szabo, L.I. Zon, J.M. Kyriakis, et al. 1996. Requirement for ceramide-initiated SAPK/JNK signalling in stress-induced apoptosis. *Nature*. 380:75–79.
14. Reed, J. 1995. Regulation of apoptosis by bcl-2 family proteins and its role in cancer and chemoresistance. *Curr. Opin. Oncol.* 7:541–546.
15. Rothstein, T.L. 1996. Signals and susceptibility to programmed death in B cells. *Curr. Opin. Immunol.* 8:362–371.
16. Nishina, H., K.D. Fischer, L. Radvanyi, A. Shahinian, R. Hakem, E.A. Rubie, A. Bernstein, T.W. Mak, J.R. Woodgett, and J.M. Penninger. 1997. Stress-signalling kinase Sek-1 protects thymocytes from apoptosis mediated by CD95 and CD3. *Science*. 275:350–353.
17. Irmeler, M., M. Thome, M. Hahne, P. Schneider, K. Hofmann, V. Steiner, J.L. Bodmer, M. Schroter, K. Burns, C. Mattmann, et al. 1997. Inhibition of death receptor signals by cellular FLIP. *Nature*. 388:190–195.
18. Resnick, D., A. Pearson, and M. Krieger. The SRCR superfamily: a family reminiscent of the Ig superfamily. *Trends Biochem. Sci.* 19:5–8.
19. Krieger, M. 1992. Molecular flypaper and atherosclerosis: structure of the macrophage scavenger receptor. *Trends Biochem. Sci.* 17:141–146.
20. Freeman, M., J. Ashkenas, D.J. Rees, D.M. Kingsley, N.G. Copeland, N.A. Jenkins, and M. Krieger. 1990. An ancient, highly conserved family of cysteine-rich protein domains revealed by cloning type I and type II murine macrophage scavenger receptors. *Proc. Natl. Acad. Sci. USA*. 87:8810–8814.
21. Shinkai, Y., G. Rathbun, K.P. Lam, E.M. Oltz, V. Stewart, M. Mendelsohn, V. Charron, M. Datta, F. Yung, A.M. Stall, and F.W. Alt. 1992. Rag-2 deficient mice lack mature lymphocytes owing to inability to initiate V(D)J rearrangement. *Cell*. 68:855–867.
22. Miyazaki, T., U. Müller, and K.S. Campbell. 1997. Normal development but differentially altered proliferative responses of lymphocytes in mice lacking CD81. *EMBO (Eur. Mol. Biol. Organ.) J.* 16:4217–4225.
23. Gilfillan, S., C. Waltzinger, C. Benoist, and D. Mathis. 1994. More efficient positive selection of thymocytes in mice lacking terminal deoxynucleotidyl transferase. *Int. Immunol.* 6:1681–1686.
24. Niwa, H., K. Yamamura, and J. Miyazaki. 1991. Efficient selection for high-expression transfectants with a novel eukaryotic vector. *Gene (Amst.)*. 108:193–199.
25. Ogasawara, J., R. Watanabe-Fukunaga, M. Adachi, A. Matsuzawa, T. Kasugai, Y. Kitamura, N. Itoh, T. Suda, and S. Nagata. 1993. Lethal effect of the anti-Fas antibody in mice. *Nature*. 364:806–809.
26. Blanden, R.V., M.J. Lefford, and G.B. Mackness. 1969. The host response to Calmette-Guérin bacillus infection in mice. *J. Exp. Med.* 129:1079–1101.
27. Kindler, V., A.P. Sappino, G.E. Grau, P.F. Piguet, and P. Vassalli. 1989. The inducing role of tumor necrosis factor in the development of bactericidal granulomas during BCG infection. *Cell*. 56:731–740.
28. Gebe, J.A., P.A. Kiener, H.Z. Ring, X. Li, U. Francke, and A. Arffo. 1997. Molecular cloning, mapping to human chromosome 1q21-q23, and cell binding characteristics of Sp α , a new member of the scavenger receptor cysteine-rich (SRCR) family of proteins. *J. Biol. Chem.* 272:6151–6158.
29. Malissen, B., and M. Malissen. 1996. Functions of TCR and pre-TCR subunits: lessons from gene ablation. *Curr. Opin. Immunol.* 8:383–393.
30. Nakayama, K., K. Nakayama, I. Negishi, K. Kuida, Y. Shinkai, M.C. Louie, L.E. Fields, P.J. Lucas, V. Stewart, and F.W. Alt. 1993. Disappearance of the lymphoid system in Bcl-2 homozygous mutant chimeric mice. *Science*. 261:1584–1588.
31. Veis, D.J., C.M. Sorenson, J.R. Shutter, and S.J. Korsmeyer.

1993. Bcl-2-deficient mice demonstrate fulminant lymphoid apoptosis, polycystic kidneys, and hypopigmented hair. *Cell*. 75:229–240.
32. Donehower, L.A., M. Harvey, B.L. Slagle, M.J. McArthur, C.A. Montgomery, Jr., J.S. Butel, and A. Bradley. 1992. Mice deficient for p53 are developmentally normal but susceptible to spontaneous tumours. *Nature*. 356:215–221.
33. Lowe, S.W., E.M. Schmitt, S.W. Smith, B.A. Osborne, and T. Jacks. 1993. p53 is required for radiation-induced apoptosis in mouse thymocytes. *Nature*. 362:847–849.
34. Clarke, A.R., C.A. Purdie, D.J. Harrison, R.G. Morris, C.C. Bird, M.L. Hooper, and A.H. Wyllie. 1993. Thymocyte apoptosis induced by p53-dependent and independent pathways. *Nature*. 362:849–852.
35. Motoyama, N., F. Wang, K.A. Roth, H. Sawa, K. Nakayama, K. Nakayama, I. Negishi, S. Senju, Q. Zhang, and S. Fujii. 1995. Massive cell death of immature hematopoietic cells and neurons in Bcl-x-deficient mice. *Science*. 267:1506–1510.
36. Ma, A., J.C. Pena, B. Chang, E. Margosian, L. Davidson, F.W. Alt, and C.B. Thompson. 1995. Bclx regulates the survival of double-positive thymocytes. *Proc. Natl. Acad. Sci. USA*. 92:4763–4767.
37. Smith, C.A., G.T. Williams, R. Kingston, E.J. Jenkinson, and J.J.T. Owen. 1989. Antibodies to CD3/T-cell receptor complex induce death by apoptosis in immature T cells in thymic cultures. *Nature*. 337:181–184.
38. Yamada, T., and H. Ohyama. 1988. Radiation-induced interphase death of rat thymocytes is internally programmed (apoptosis). *Int. J. Radiat. Biol.* 53:251–259.
39. King, L.B., M.S. Vacchio, R. Hunziker, D.H. Margulies, and J.D. Ashwell. 1995. A targeted glucocorticoid receptor antisense transgene increases thymocyte apoptosis and alters thymocyte development. *Immunity*. 3:647–656.
40. Linette, G.P., and S.J. Korsmeyer. 1994. Differentiation and cell death: lessons from the immune system. *Curr. Opin. Cell Biol.* 6:809–815.
41. Linette, G.P., M.J. Grusby, S.M. Hedrick, T.H. Hansen, L.H. Glimcher, and S.J. Korsmeyer. 1994. Bcl-2 is upregulated at the CD4⁺ CD8⁺ stage during positive selection and promotes differentiation at several control points. *Immunity*. 1:197–205.
42. Tao, W., S.J. Teh, I. Melhado, F. Jirik, S.J. Korsmeyer, and H.S. Teh. 1994. The T cell receptor repertoire of CD4⁻ CD8⁺ thymocytes is altered by overexpression of the Bcl-2 protooncogene in the thymus. *J. Exp. Med.* 179:145–153.
43. Itoh, N., S. Yonehara, A. Ishii, M. Yonehara, S. Mizushima, M. Sameshima, A. Hase, Y. Seto, and S. Nagata. 1991. The polypeptide encoded by the cDNA for human cell surface antigen Fas can mediate apoptosis. *Cell*. 66:233–243.
44. Kyewski, B.A., F. Momburg, and V. Schirmacher. 1987. Phenotype of stromal cell-associated thymocytes in situ is compatible with selection of the T cell repertoire at an “immature” stage of thymic T cell differentiation. *Eur. J. Immunol.* 17:961–967.
45. Kyewski, B.A. 1987. Seeding of thymic microenvironments defined by distinct thymocyte–stromal cell interactions is developmentally controlled. *J. Exp. Med.* 166:520–538.
46. Kyewski, B.A., V. Schirmacher, and J. Allison. 1989. Antibodies against the T cell receptor/CD3 complex interfere with distinct intra-thymic cell-cell interactions in vivo: correlation with arrest of T cell differentiation. *Eur. J. Immunol.* 19:857–863.
47. Aliprantis, A.O., G. Diez-Roux, L.C. Mulder, A. Zychlinsky, and R.A. Lang. 1996. Do macrophages kill through apoptosis? *Immunol. Today*. 17:573–576.